Available online at https://li02.tci-thaijo.org/index.php/ssstj

Suan Sunandha Science and Technology Journal

Investigation of Charged Particles Interaction with $CeBr_3$ Scintillator by Monte Carlo Simulation Programs

Chalermpon Mutuwong[1], Wuttichai Chaiphaksa[2,3*], Jakrapong Kaewkhao[2,3], Cherdsak Bootjomchai[1]

[1]Department of Physics, Faculty of Science, Ubon Ratchathani University, Warin Chamrap,Ubon Ratchathani 34190, Thailand
[2]Physics Program, Faculty of Science and Technology, Nakhon Pathom Rajabhat University, Nakhon Pathom 73000, Thailand
[3]Center of Excellence in Glass Technology (CEGM), Nakhon Pathom Rajabhat University, Nakhon Pathom 73000, Thailand
***Corresponding author e-mail: wuttichai@npru.ac.th**

Received: *28 August 2023* / **Revised:** *14 November 2023* / **Accepted:** *15 December 2023*

Abstract
This work aims to investigate the interaction of charged particles (alpha and proton) with the $CeBr_3$ scintillator by using Monte Carlo simulation. The total mass stopping power (TMSP), projected range, ion distributions, and ion ranges in the $CeBr_3$ at an energy range of 0.01 MeV - 10,000 MeV, were computed by SRIM and FLUKA programs. The simulation results show that the TMSP of CeBr3 obtained by both programs is in good agreement. The alpha particle has a higher TMSP of the $CeBr_3$ than the proton. The projected range of alpha and proton particles increases with increasing energy. The projected range of the proton is higher than that of the alpha particle when compared at the same energy. Finally, the 2D visualization of ion distributions and ion ranges for alpha and proton particles was reported.

Keywords: $CeBr_3$ scintillator, Monte Carlo simulation, Alpha, Proton

1. Introduction

Scintillators are materials that can emit visible light when interacting with radiation. Nowadays, scintillators have been continually used in industrial, medical, and scientific applications. Inorganic scintillators such as $CeBr_3$ are interesting due to high density and high-energy resolution of gamma-ray spectroscopy at room temperature (Idoeta, Herranz, Alegría, & Legarda, 2021). In recent years, many researchers have examined the fundamental characteristics of $CeBr_3$ detectors such as energy resolution (Naqvi, Khiari, Liadi, Khateeb-ur-Rehman, & Isab, 2016), pulse linearity (Giaz et al., 2015) and timing properties (Swiderski, Moszynski, Syntfeld-Kazuch, Szawlowski, & Szczesniak, 2014). There is no information on charged particles interacting with $CeBr_3$ scintillators. Therefore, this work aims to study charged particles interacting with $CeBr_3$ scintillators by using Monte Carlo simulation programs.

2. Theory

2.1 Mass stopping power

When the charged particles pass through matter, they lose energy by transferring their energy to excite and ionize the atoms or molecules of matter. The properties of materials that cause charged particles to lose energy per depth per density is called "Mass stopping power", as described by the Bethe-Bloch formula (Braibant, Giacomelli, & Spurio, 2012):

$$-\frac{1}{\rho}\frac{dE}{dx} = 2\pi N_A m_e r_e^2 c^2 \frac{Z}{A}\frac{z_e^2}{\beta^2}\left[\ln\left(\frac{2m_e\gamma^2 v^2 W_{max}}{I^2}\right) - 2\beta^2 - \delta - 2\frac{C}{Z}\right] \quad (1)$$

where

$r_e = e^2/m_e c^2$ classical electron radius
$2\pi m_e r_e^2 c^2$ = 0.1535 MeV $g^{-1}cm^2$

m_e= electron mass = $9.110 \cdot 10^{-31}$ kg
N_A = Avogadro's number = $6.022 \cdot 10^{23}$ mol^{-1}
I = mean ionization(*excitation*) potential of target
ρ = material density
Z = atomic number of absorber medium
A = atomic weight of absorber medium
z_e= charge of the incident particle
$\beta = v/c$ of incident particle
$\gamma = 1/\sqrt{1-\beta^2}$
δ = density effect correction (vital at high energy)
C = shell correction (already vital at low energy)
W_{max} = maximum kinetic energy imparted to an e^- in a single collision $\cong 2m_e c^2(\beta\gamma)^2$, for $M \gg m_e$.

2.2 Monte Carlo simulation software

Monte Carlo method is one of the old and most effective techniques for solving generally complex problems involving particle transport and interactions with matter in complex geometries (Ahdida et al., 2022). Nowadays, the software based on this methodology, such as FLUKA (Battistoni et al., 2015), GEANT4 (Allison et al., 2016), MCNPX (Vahabi & Shamsaie Zafarghandi, 2020), PHITS (Sato et al., 2018), and SRIM (Ziegler, Ziegler, & Biersack, 2010), has been widely used to simulate the particle transport and interactions with matter. In this work, the charged particles interaction with $CeBr_3$ scintillators were investigated by SRIM and FLUKA Monte Carlo simulation programs. The weight fraction, and density of $CeBr_3$ are Ce(0.3689) and Br(0.6311), and 5.2 g/cm^3, respectively. The SRIM and FLUKA were used to calculate the total mass stopping power (TMSP) of the $CeBr_3$ for alpha and proton particles in the energy range of 0.01 MeV – 10,000 MeV. Moreover, the projected range, ion distribution, and ion ranges of the $CeBr_3$ for alpha and proton particles were investigated by SRIM. The simulation was run with a total of 10,000 primary particles.

3. Results and Discussion

The TMSP, projected range, ion distribution, and ion ranges of the $CeBr_3$ scintillator for alpha and proton particles were investigated using SRIM and FLUKA programs. The TMSP of $CeBr_3$ in energy range of 0.01 MeV- to 10,000 MeV for a) alpha and b) proton was illustrated in Figure 1.

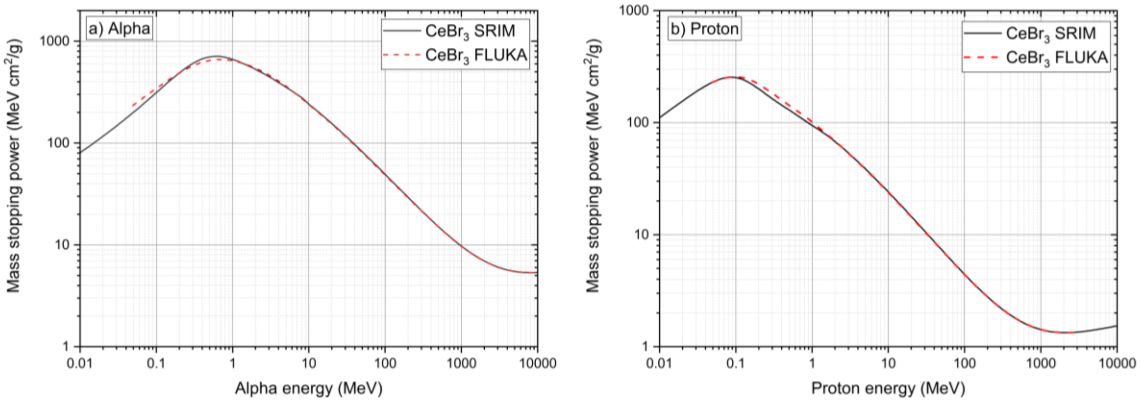

Figure 1. Mass stopping power of $CeBr_3$ for a) alpha and b) proton particles in energy ranges from 0.01 MeV to 10,000 MeV computed by SRIM (solid line) and FLUKA (dashed line).

The results found that the TMSP of the $CeBr_3$ scintillator computed by SRIM and FLUKA is in good agreement. The maximum values of TMSP are approximately 711.50 MeV cm^2/g at an alpha energy of 0.65 MeV and 256.35 MeV cm^2/g at a proton energy of 0.10 MeV, respectively. Due to the energy dependence of the energy loss (or total mass stopping power curve), incoming high-energy particles experience a negligible energy loss dE/dx, whereas the energy loss reaches its maximum when the particles have slowed to energies that correspond to the peak of the energy loss curve (El-Ghossain, 2017). In addition, the TMSP of the alpha particle tends to be higher than that of the proton as increasing energy. This effect is a result of the fact that the alpha particle has a lower penetration power than the proton. This is because the TMSP value of alpha particle is more than that of proton particle. The TMSP indicates the potentiality of a material to reduce the kinetic energy of particles traveling toward it by ionizing the molecules. The average penetration depth that particles stop in the material is called the "projected range".

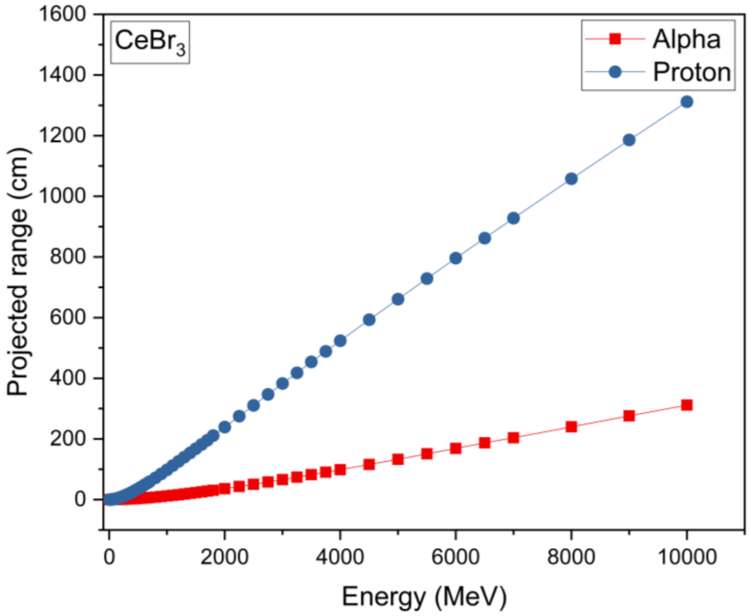

Figure 2. The projected range of alpha and proton particles in $CeBr_3$ from 0.01 MeV to 10,000 MeV.

Error! Reference source not found.The average penetration depth of alpha and proton into $CeBr_3$ as a function of their kinetic energy was shown in Figure 2. The results indicate that the projected range of alpha and proton particles penetrating the $CeBr_3$ increases with increasing energy. Moreover, because proton particles have greater penetration power than alpha particles, the projected range of the proton particles is greater than that of the alpha particles when compared with the same energy.

The 2D simulation of the ion distribution when alpha particles interact with $CeBr_3$ at energies of a) 0.01 MeV and b) 0.05 MeV is shown in Figure 3a and 3b, respectively. The alpha particles lose their energy by transferring energy to $CeBr_3$. The alpha particle has enough energy to ionize the Ce and Br atoms. These ions and alpha still move into $CeBr_3$ until their movement are stopped. The orange line traces the Ce ion trajectory until it stops at the green dot. The blue line traces the movement path of the Br ion until it stops at the purple dot. The black line is the trajectory of alpha particles to stop in $CeBr_3$ at the red dot. The simulation results showed the ion range distribution of alpha particles into $CeBr_3$ is between 0 angstrom and 0.28 µm for incident alpha energies of 0.01 MeV (Figure 3c) and between 0 angstrom and 0.84 µm for incident energies of 0.05 MeV (Figure 3d). The average ion ranges of alpha particles are about 916 angstroms or 0.0916 µm for 0.01 MeV, as shown in Figure 3c, and about 3525 angstroms or 0.3525 µm for 0.05 MeV, as illustrated in Figure 3d.

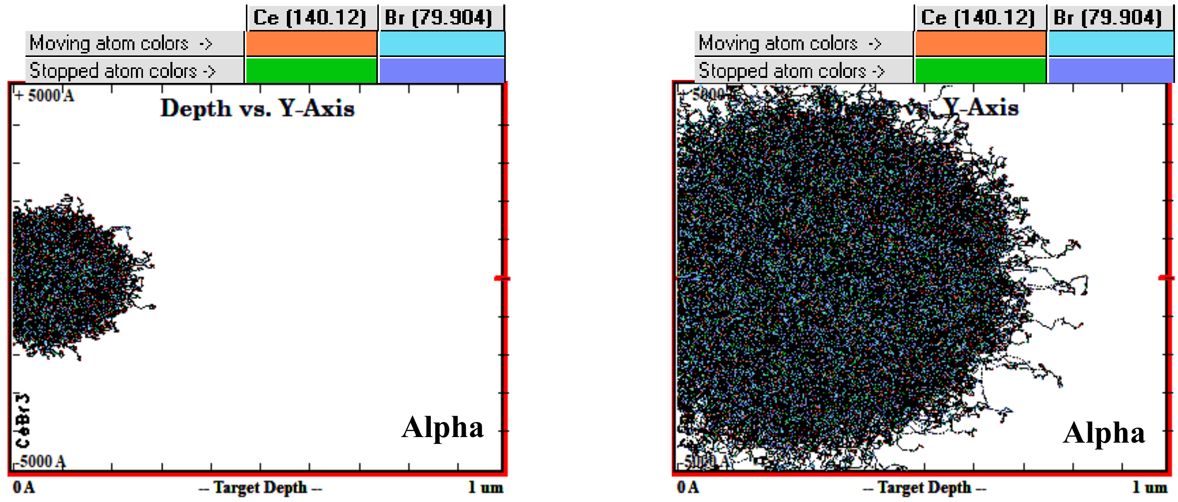

a) 0.01 MeV b) 0.05 MeV

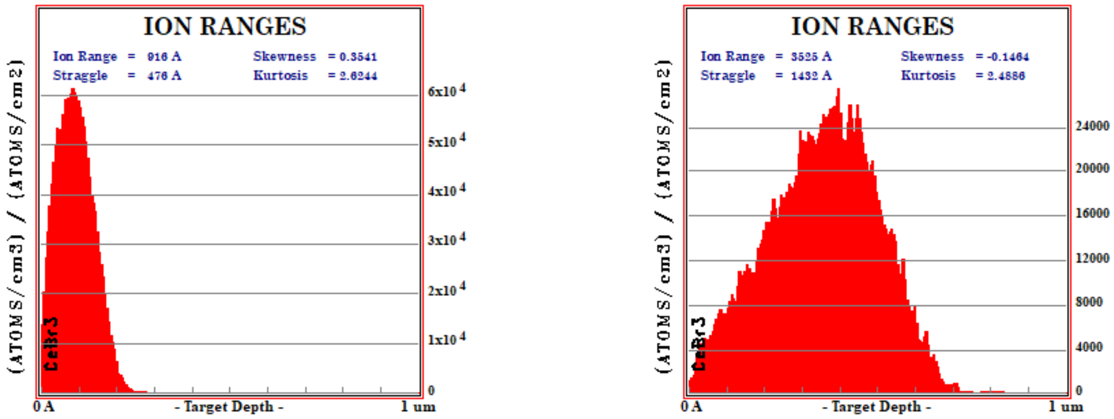

c) 0.01 MeV d) 0.05 MeV

Figure 3. The 2D Monte Carlo simulation of the 10,000 alpha particles interact with the $CeBr_3$ at energies a) 0.01 MeV, b) 0.05 MeV, and the probability distributions of ion ranges at c) 0.01 MeV and d) 0.05 MeV.

The results of the 2D simulation of the ion distribution produced by proton particle interactions with $CeBr_3$ at energies of 0.01 MeV and 0.05 MeV were shown in Figure 4a and 4b, respectively. According to the simulation results, the ion range distribution of proton particles into $CeBr_3$ is between 0 angstrom and 0.30 µm for incident energies of 0.01 MeV (Figure 4c) and between 0 angstrom and 0.74 µm for incident energies of 0.05 MeV (Figure 4d). The average penetration depth of proton particles is about 1168 angstroms or 0.1168 µm for 0.01 MeV, as shown in Figure 4c, and about 4224 angstroms or 0.4224 µm for 0.05 MeV, as shown in Figure 4d.

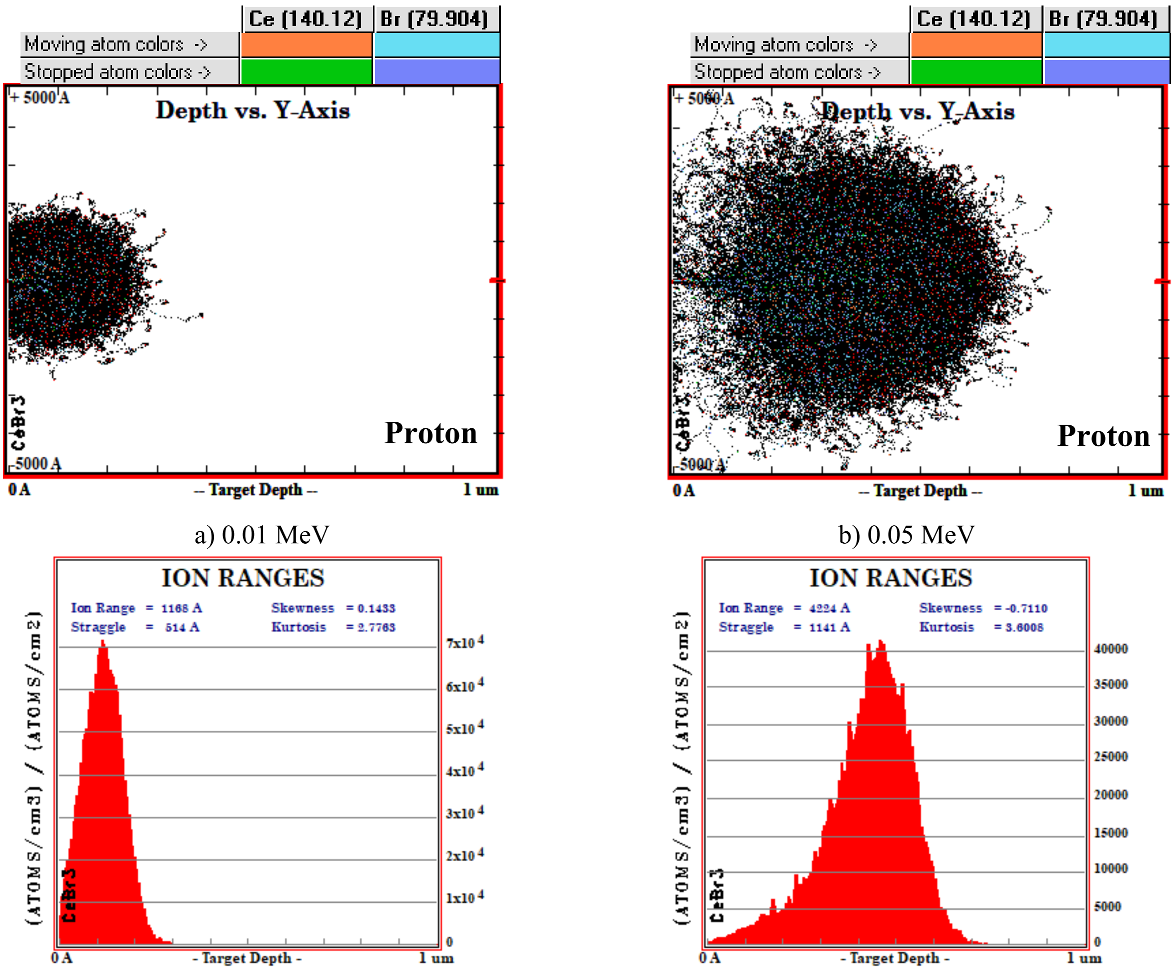

c) 0.01 MeV d) 0.05 MeV

Figure 4. The 2D Monte Carlo simulation of the 10,000 proton particles interact with the $CeBr_3$ at energies a) 0.01 MeV, b) 0.05 MeV, and the probability distributions of ion ranges at c) 0.01 MeV and d) 0.05 MeV.

4. Conclusion

The TMSP, projected range, ion distribution, and ion ranges of alpha and protons interacting with the $CeBr_3$ scintillator in the energy range of 0.01 MeV - 10,000 MeV were studied by using SRIM and FLUKA software. The results found that the TMSP of the $CeBr_3$ scintillator for alpha and proton is in excellent agreement. The TMSP of the alpha particle tends to be higher than that of the proton. The projected range of alpha particles and protons in the $CeBr_3$ increases with increasing energy. The projected range of the proton is higher than that of the alpha particle when at the same energy. Finally, the 2D simulation of ion distributions and ion ranges for alpha and proton particles was reported. The average ion ranges of alpha particles are 0.0916 µm for 0.01 MeV and 0.3525 µm for 0.05 MeV. For proton particles, the average ion ranges are 0.1168 µm for 0.01 MeV and 0.4224 µm for 0.05 MeV.

Acknowledgements

The authors would like to thank National Research Council of Thailand (NRCT) through the Research and Researchers for Industries (RRI) Ph.D. Program (NRCT5-RRI63015-P19) for funding this research. The authors express gratitude Thailand Science Research and Innovation (TSRI) for support supporting this research (Project number TSRI_66_9.2).

References

Ahdida, C., Bozzato, D., Calzolari, D., Cerutti, F., Charitonidis, N., Cimmino, A., ... Widorski, M. (2022). New capabilities of the FLUKA multi-purpose code. *Frontiers in Physics*, *9*, 788253. doi:10.3389/fphy.2021.788253

Allison, J., Amako, K., Apostolakis, J., Arce, P., Asai, M., Aso, T., … Yoshida, H. (2016). Recent developments in GEANT4. *Nuclear Instruments and Methods in Physics Research, Section A: Accelerators, Spectrometers, Detectors and Associated Equipment*, *835*, 186-225. doi:10.1016/j.nima.2016.06.125

Battistoni, G., Boehlen, T., Cerutti, F., Chin, P. W., Esposito, L. S., Fassò, A., ... Smirnov, G. (2015). Overview of the FLUKA code. *Annals of Nuclear Energy*, *82*, 10-18. doi:10.1016/j.anucene.2014.11.007

Braibant, S., Giacomelli, G., & Spurio, M. (2012). *Particles and fundamental interactions*. Dordrecht: Springer.

El-Ghossain, M. O. (2017). Calculations of stopping power, and range of ions radiation (alpha particles) interaction with different materials and human body parts. *International Journal of Physics*, *5*(3), 92-98.

Giaz, A., Hull, G., Fossati, V., Cherepy, N., Camera, F., Blasi, N., ... Riboldi, S. (2015). Preliminary investigation of scintillator materials properties: SrI_2:Eu, $CeBr_3$ and GYGAG:Ce for gamma rays up to 9 MeV. *Nuclear Instruments and Methods in Physics Research Section A: Accelerators, Spectrometers, Detectors and Associated Equipment*, *804*, 212-220. doi:10.1016/j.nima.2015.09.065

Idoeta, R., Herranz, M., Alegría, N., & Legarda, F. (2021). Possibilities of the use of $CeBr_3$ scintillation detectors for the measurement of the content of radionuclides in samples for environmental monitoring. *Applied Radiation and Isotopes*, *176*. doi:10.1016/j.apradiso.2021.109881

Naqvi, A. A., Khiari, F. Z., Liadi, F. A., Khateeb-ur-Rehman, & Isab, A. A. (2016). Performance tests of a large volume cerium tribromide ($CeBr_3$) scintillation detector. *Applied Radiation and Isotopes*, *114*, 50-56. doi:10.1016/j.apradiso.2016.04.031

Sato, T., Iwamoto, Y., Hashimoto, S., Ogawa, T., Furuta, T., Abe, S. I., ... Niita, K. (2018). Features of particle and heavy ion transport code system (PHITS) version 3.02. *Journal of Nuclear Science and Technology*, *55*(6), 684-690. doi:10.1080/00223131.2017.1419890

Swiderski, L., Moszynski, M., Syntfeld-Kazuch, A., Szawlowski, M., & Szczesniak, T. (2014). Measuring the scintillation decay time for different energy depositions in NaI:Tl, LSO:Ce and $CeBr_3$ scintillators. *Nuclear Instruments and Methods in Physics Research Section A: Accelerators, Spectrometers, Detectors and Associated Equipment*, *749*, 68-73. doi:10.1016/j.nima.2014.02.045

Vahabi, S. M., & Shamsaie Zafarghandi, M. (2020). Applications of MCNP simulation in treatment planning: A comparative study. *Radiation and Environmental Biophysics*, *59*(2), 307-319. doi:10.1007/s00411-020-00841-2

Ziegler, J. F., Ziegler, M. D., & Biersack, J. P. (2010). SRIM–The stopping and range of ions in matter (2010). *Nuclear Instruments and Methods in Physics Research Section B: Beam Interactions with Materials and Atoms*, *268*(11-12), 1818-1823. doi:10.1016/j.nimb.2010.02.091